Head and Neck Pathology (2022) 16:679–694
https://doi.org/10.1007/s12105-022-01412-1

ORIGINAL PAPER

# Adamantinoma-Like Ewing Sarcoma of the Head and Neck: A Case-Series of a Rare and Challenging Diagnosis

**Munita Bal[1] · Aekta Shah[1] · Bharat Rekhi[1] · Neha Mittal[1] · Swapnil Ulhas Rane[1] · Katha Rabade[1] · Omshree Shetty[2] · Gouri Pantavaidya[3] · Deepa Nair[3] · Kumar Prabhash[4] · M. Aishwarya[5] · Krishan Kumar Govindarajan[5] · Siddhartha Laskar[6] · Sarbani Ghosh Laskar[6] · Asawari Patil[1]**

Received: 22 November 2021 / Accepted: 3 January 2022 / Published online: 13 January 2022


## Abstract

Adamantinoma-like Ewing sarcoma (ALES) is a rare malignant tumor characterized by *EWSR1::FLI1* related fusions and complex epithelial differentiation. ALES poses a tremendous diagnostic challenge owing to its resemblance to a wide variety of common head and neck malignancies. We aimed to study the clinicopathologic spectrum of ALES diagnosed at our institute. A retrospective review of the clinical and pathologic features of all *EWSR1*-rearranged ALES cases was performed after confirming the diagnosis. The cases lacking *EWSR1* rearrangement were excluded. A total of 7 patients were analyzed. The median age was 27 years (range 7–42 years). There were 4 males and 3 female patients. Tumors were distributed as follows: maxilla (n = 2), parotid (n = 2), nasal cavity (n = 1), ethmoid/maxilla (n = 1), and thyroid (n = 1). Tumor size ranged from 2.2 to 5.5 cm. On microscopy, tumors displayed nested-lobular architecture, monomorphic cells, and interlobular fibrotic stroma. Other features included: palisading (n = 5), squamous differentiation (n = 2), keratinization (n = 1), colonisation of salivary ducts (n = 1) and thyroid follicles (n = 1), follicle-like cysts (n = 3), calcification (n = 2), necrosis (n = 3). Mitotic rate was 4–15/2 $mm^2$. On immunohistochemistry, cytokeratins (100%), p40 (100%), strong/diffuse membranous CD99 (100%), NKX2.2 (100%), Fli-1 (71%), and synaptophysin (71%) was positive. Patients received chemotherapy (n = 7) and radiotherapy (n = 4). Two patients developed recurrence at 6 and 10 months; 3 developed metastases at 0, 6, and 25 months. ALES is a rare and aggressive malignancy that mimics diverse neoplasms common in the head and neck region. Awareness of the morphologic and immunohistochemistry spectrum of this tumor is essential to avoid diagnostic errors.

**Keywords** Adamantinoma-like Ewing sarcoma · Head and neck · Salivary · Thyroid · Sinonasal · Orbit · Pathology · Ewing sarcoma · EWSR1 · Undifferentiated round cell sarcomas · Treatment · Clinical

## Introduction

Adamantinoma-like Ewing sarcoma (ALES) is a rare malignant tumor characterized by *EWSR1::FLI1* translocation and complex epithelial differentiation. First described by Bridge et al. [1], ALES is currently regarded as a variant of Ewing sarcoma on account of shared round cell morphology, CD99 (mic2) and NKX2.2 immunoreactivity, and the genetic hallmark of *EWSR1::FLI1* fusion [2]. While up to 25–30% of classical Ewing sarcomas may exhibit epithelial

✉ Munita Bal
munitamenon@gmail.com

1 Department of Pathology, Tata Memorial Centre, Homi Bhabha National Institute, Mumbai, Maharashtra, India

2 Division of Molecular Pathology and Translational Medicine, Tata Memorial Centre, Homi Bhabha National Institute, Mumbai, Maharashtra, India

3 Department of Surgical Oncology, Tata Memorial Centre, Homi Bhabha National Institute, Mumbai, Maharashtra, India

4 Department of Medical Oncology, Tata Memorial Centre, Homi Bhabha National Institute, Mumbai, Maharashtra, India

5 Department of Pediatric Surgery, Jawaharlal Institute of Postgraduate Medical Education and Research, Pudducherry, India

6 Department of Radiation Oncology, Tata Memorial Centre, Homi Bhabha National Institute, Mumbai, Maharashtra, India

differentiation, the keratin expression is usually limited and seen with low-molecular-weight cytokeratins [2]. In contradistinction, ALES displays diffuse immunoreactivity with p40/p63 and high-molecular-weight cytokeratins, with a subset exhibiting overt squamous differentiation and even keratin pearl formation, that quite set them apart from the classical Ewing sarcoma [3].

Initially described in the extremities, a striking proportion (74%) of ALES cases show a predilection for the head and neck region [3]. Nonetheless, ALES is a rare entity with only 28 head and neck cases reported to date [3–18]. While ALES diagnosis is challenging at all sites, occurrence in the head and neck poses additional difficulties as the presence of squamous differentiation or immunohistochemical epithelial reactivity can be mistaken for an epithelial malignancy. Owing to its rarity, little information is available on the clinical course as well as the optimal treatment of ALES, although reports hint at outcomes similar to or a slightly more favorable one than Ewing sarcoma after treatment with surgery, adjuvant chemotherapy, and radiotherapy [3]. Herein, we report seven cases of ALES arising in the head and neck and complement it with a review of the literature to underscore their distinguishing features and clinical behavior.

## Materials and Methods

Clinical and pathologic data of all cases of ALES arising in the head and neck region were retrieved from the archives of the Department of Pathology at our tertiary-care oncology institute. The key words used for search were: 'adamantinoma-like,' 'Ewing family of tumors', 'ALES', 'undifferentiated round cell sarcoma', 'Ewing sarcoma', 'atypical Ewing sarcoma', 'Ewing sarcoma with epithelial differentiation'. Hematoxylin & eosin-stained slides and immunohistochemistry (IHC) slides of all cases were reviewed and the diagnosis was reconfirmed [2].

Data on age, sex, symptomatology, tumor location, treatment details, local recurrence, metastasis, and the status at the last follow-up visit were recorded from the hospital's electronic medical records. Pathologic features recorded were: tumor size, architectural pattern, cellular characteristics, epithelial differentiation (identified on IHC), squamous differentiation (morphologically recognizable as squamous cells), keratinization, stromal characteristics, mucosal surface involvement/ pagetoid spread, mitotic figure count (per 2 $mm^2$), necrosis, lymphovascular invasion (LVI), perineural invasion (PNI), resection margins, lymph node (LN) status, and IHC profile.

Immunostaining was performed on a Benchmark XT autostainer (Ventana) using the MACH2 Ultraview polymer detection kit (Ventana) and included appropriate controls. The list of antibodies, clones, and dilutions used in the cases has been listed in the Supplementary table.

Fluorescence in-situ hybridization (FISH) for *EWSR1* rearrangements was performed using LSI break apart, dual-color *EWSR1* probe (Zytolight SPEC *EWSR*1 dual-color break-apart probe) consisting of two DNA probes: the first, a ~ 500 kb probe labeled in Spectrum Orange, flanking the 5` side of the *EWSR1* gene; the second, a ~ 1100 kb probe labeled in Spectrum Green, flanking the 3` side of the *EWSR1* gene. This probe kit can detect *EWSR1* gene rearrangements involving the known breakpoints restricted to introns 7 through 10. The processed sections were stained with 4′-6-Diamidino-2-phenylindole (DAPI) and examined under a fluorescent microscope (Carl Zeiss, Axio Imager Z1, Germany), using AxioCam MRc5 camera and Axio vision Rel 4.5 software. The signals were manually scored and the tumor was considered positive if more than 15% of 100 cells analyzed showed a split signal/ break-apart. Molecular tests, by the FISH technique in all cases were reported by two authors (OS and BR).

## Results

A total of ten patients with a diagnosis of head and neck ALES were identified. Out of these, two cases (sinonasal, and parotid) while showing malignant round cell morphology, strong and membranous CD99, diffuse AE1/AE3 and p40 positivity, were found to lack *EWSR1* gene rearrangements on the FISH assay. For the third patient (peri-orbital), since the tissue was inadequate and the patient refused surgery, molecular confirmation was not possible. These three cases were excluded from the study. One patient with confirmed *EWSR1* rearrangement using break-apart FISH testing done in an outside NABL-accredited laboratory was included. Hence, a total of 7 patients with *EWSR1*-rearranged ALES were included in the present study. Of these, six patients had been referred with a different initial diagnosis before presenting at our institute; these included: basaloid squamous cell carcinoma (SCC) (n = 2), sialoblastoma (n = 1), basal cell adenocarcinoma (n = 1), poorly differentiated thyroid carcinoma (n = 1); 1 patient (case 6) was diagnosed as solid pseudopapillary tumor of the pancreas (n = 1) on pancreatic biopsy. Diagnoses in these 6 cases were revised to ALES after review at our institute.

### Clinical Findings

The details of the clinical findings of ALES patients are provided in Table 1. Briefly, the tumors were distributed in the sinonasal tract (n = 4), parotid (n = 2), and the thyroid (n = 1). The median age was 27 years with a male-to-female ratio of 1.3. The initial presentations were largely related to

**Table 1** Clinical features of Adamantinoma-like Ewing Sarcoma cases (n = 7)

| Features | Case 1 | Case 2 | Case 3 | Case 4 | Case 5 | Case 6 | Case 7 |
|---|---|---|---|---|---|---|---|
| Age | 7 y/M | 12 y/F | 42/M | 30 y/M | 27 y/M | 25/F | 34/F |
| Site | Thyroid | Parotid | Parotid | Nasal cavity | Maxilla | Maxilla | Ethmoid/maxilla |
| Symptoms | Swelling | Mass | Swelling | Obstruction, epistaxis | Obstruction, pain | Abdominal pain | Headache |
| Surgery | Hemi thyroidectomy | Parotidectomy | Lt adequate parotidectomy | Rhinectomy + premaxilla ectomy + BL ND | Rt total Maxillectomy + SND | No | Ethmoidectomy |
| Radiotherapy | No | Yes (55.8 Gy/31# (@1.8 Gy/#) | No | Yes (45 Gy/ 25#/ 5 weeks) | Yes (55.8 Gy / 31 #) | Yes (Palliative RT for skeletal metastasis) | No |
| Chemotherapy | Yes (EFT 2001 protocol) | Yes (EFT 2001 protocol) | No (defaulted) | Yes (defaulted post RT; received VAC-IE 6 cycles at recurrence10 months later) | Yes (COG Induction protocol VAC/IE; consolidation with VAC/IE post RT) | Yes (EFT 2001) | Yes (VAC/IE) |
| Follow-up (duration) | 32 months | 26 months | NA | 39 months | 4 months | 24 months | 0 |
| Recurrence | No | No | NA | Yes | Yes | No | No |
| Distant metastasis | Yes | No | NA | Yes | No | Yes | No |
| Status at last follow-up | AWD | ANED | NA | AWD (progressive disease) | ANED | AWD (progressive disease) | Ongoing treatment |

*M* male, *F* female, *Rt* right, *Lt* left, *BL ND* bilateral neck dissection, *SND* selective neck dissection, *RT* radiotherapy, *Gy* Gray, *COG* Children Oncology Group, *VAC/IE* alternating vincristine + doxorubicin + cyclophosphamide and ifosfamide + etoposide, *NA* not available, *AWD* alive with disease, *ANED* alive with no evidence of disease

the tumor location: the patients with the parotid and thyroid tumors presented with a painless growing mass/swelling (n = 3) while the sinonasal tumors presented with epistaxis and nasal obstruction (n = 2), and persistent headaches (n = 1). Case 6 initially presented with recalcitrant abdominal pain and on evaluation was found to have disseminated malignancy with skeletal and pancreatic metastases. On examination, a tumor in the maxilla, presenting as an upper gingivobuccal proliferative mass, was found. Based on the mucosal involvement and the largest mass on imaging, the tumor was regarded as a maxillary primary in a multidisciplinary clinic. Six patients (except case 6) underwent surgical resection of their tumors.

## Pathologic Features

The pathologic characteristics of ALES are detailed in Table 2 and illustrated in Figs. 1, 2, 3, and 4. Briefly, the average tumor size was 3.9 cm (range, 2.2–5.5 cm). Macroscopy findings for sinonasal tumors were recorded as fleshy, homogenous, and grey-white. The thyroid tumor (case 1) was circumscribed nodular mass with a homogenous grey-white cut surface and lacking extrathyroidal spread. Both the parotid tumors were also grossly well-delineated and without extra-parenchymal spread.

On microscopy, while the tumors appeared relatively circumscribed at low power, the tumor edges revealed an infiltrative interface in all cases. At low magnification, all tumors displayed nests and lobules composed of closely packed blue round cells and separated by hyalinized stroma (Fig. 1). Higher magnification revealed round to epithelioid cells with fine chromatin, inconspicuous nucleoli, and negligible to scant pale cytoplasm that imparted a round cell (n = 4) or a basaloid (n = 3) appearance to the tumors (Fig. 2A, B). Nonetheless, tumor cells were conspicuous for their cellular monotony (Fig. 2A, B). Pseudo-rosettes were identified focally in 2 cases. At places, a few tumor nests exhibited peripheral palisading that was conspicuous in 2, focal in 3, and absent in 2 cases (Fig. 2C). While the nested architecture was characteristic, two cases revealed areas where nests coalesced to form solid sheets (Fig. 1C). Remarkably, the vestiges of original nests were still apparent within the tumor sheets due to a 'clefting artifact' outlining the merging nests (Fig. 3I).

Overt squamous differentiation was identified in 2 cases, visible as pink spots on low power in an otherwise blue

**Table 2** Pathologic features of Adamantinoma-like Ewing Sarcoma cases (n = 7)

| Features | Case 1 | Case 2 | Case 3 | Case 4 | Case 5 | Case 6 | Case 7 |
|---|---|---|---|---|---|---|---|
| Site | Thyroid | Parotid | Parotid | Nasal cavity | Maxilla | Maxilla | Ethmoid/maxilla |
| Initial diagnosis | Poorly differentiated thyroid carcinoma | Sialoblastoma | Basal cell adenocarcinoma | Basaloid SCC | Basaloid SCC | Round cell tumor/solid pseudopapillary tumor | ALES |
| Tumor size (cms) | 3.7 | 3.3 | 2.2 | 5 | 5.5 | 3.6* | 4.3 |
| Cell morphology | Round | Round | Basaloid | Round | Basaloid | Round | Round |
| Cellular appearance | Monotonous | Monotonous | Monotonous | Monotonous | Monotonous | Monotonous | Monotonous |
| Architecture | Nested | Sheets and nests | Nested-lobular | Nested-lobular, focally trabecular | Nested focally; sheets with fibrous bands | Nested | Nested |
| Rosettes | Focal | Absent | Absent | Absent | Focal | Absent | Absent |
| Palisading# | Focal | Focal | Focal | Present | Present | Absent | Absent |
| Squamous | Absent | Absent | Present; abrupt | Present; abrupt | Absent | Absent | Absent |
| Keratinization | Absent | Absent | Present | Absent | Absent | Absent | Absent |
| Calcification | Present | Absent | Present | Absent | Absent | Absent | Absent |
| Follicle-like spaces | Present | Present | Absent | Present | Absent | Absent | Absent |
| Stroma | Hyalinised | Minimal; thin fibrovascular septae | Fibrotic | Hyalinized | Fibrous bands; focally myxoid | Loose edematous | Hyalinized |
| Colonization | Present | Present | Absent | Absent | Absent | Absent | Absent |
| Mitotic rate/2mm$^2$ | 4 | 5 | 15 | 12 | 7 | 12 | 6 |
| Necrosis | Present; min | Absent | Present | Absent | Absent | Present | Absent |
| Lymphovascular invasion | Absent | Absent | Absent | Absent | Absent | Absent | Absent |
| Perineural invasion | Absent | Absent | Present | Absent | Absent | Absent | Absent |
| R status | R0 | R0 | R1 | R0 | R1 | NA | R0 |
| Underlying bone | NA | NA | NA | Cartilage involved | Involved | NA | Involved |
| Lymph nodes metastasis | Clinically node negative | Negative (0/3) | Negative (0/1) | Negative | Negative (0/29) | Not done | Clinically node negative |

*SCC* squamous cell carcinoma, *ALES* Adamantinoma-like Ewing sarcoma, *min* minimal, *R status* resection margins status, *R0* negative margins, *R1* microscopically positive margins, *NA* not available

*Tumor size on imaging

# focal- < 50% of the tumor

tumor. In the parotid (case 3), squamous nests, eddies as well as larger keratinized squamous pearls were identified centered abruptly within the monotonous round cells (Fig. 3A–D). Many of the keratinous pearls were calcified. In the second tumor (case 4), the squamous nests were less frequent, smaller, and non-keratinized. Peculiar colonization, rather than destructive infiltration, by tumor cells, was noted (case 1, 2). While in the parotid, tumor cells were seen creeping along and replacing the salivary ducts and the acini (keeping their architecture intact (Fig. 3F–G), the colonizing pattern of spread in the thyroid was more striking. Solid nests of tumor cells were admixed with intact thyroid follicles displaying variably thick collars of neoplastic cells replacing normal follicular cells in a clinging pattern while retaining luminal (colloid) secretions (Figs. 1D, 2F, 3E). Notably, similar follicle-like spaces filled with pale eosinophilic fluid were identified punctuating tumor nests and sheets in two non-thyroidal tumors (Fig. 2D–E). Entrapped ducts were noted in 1 case. Interlobular tumor stroma was hyalinized stroma in the majority while in others it was

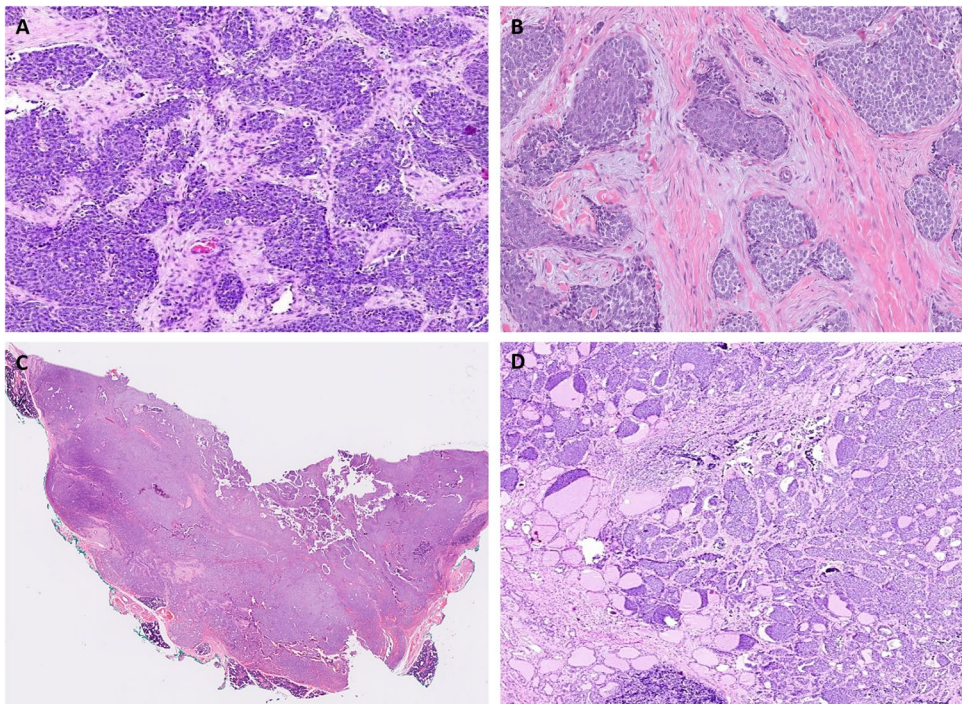


**Fig. 1** ALES typically displayed lobules and nests of closely packed blue round cells separated by hyalinized stroma (**A**, **B**). Infrequently, diffuse cellular sheets with fewer nests were identified in the parotid (case 2; **C**). In the thyroid (case 1), the tumor revealed a nested architecture with a striking colonizing pattern of spread recognizable at low power (**D**)

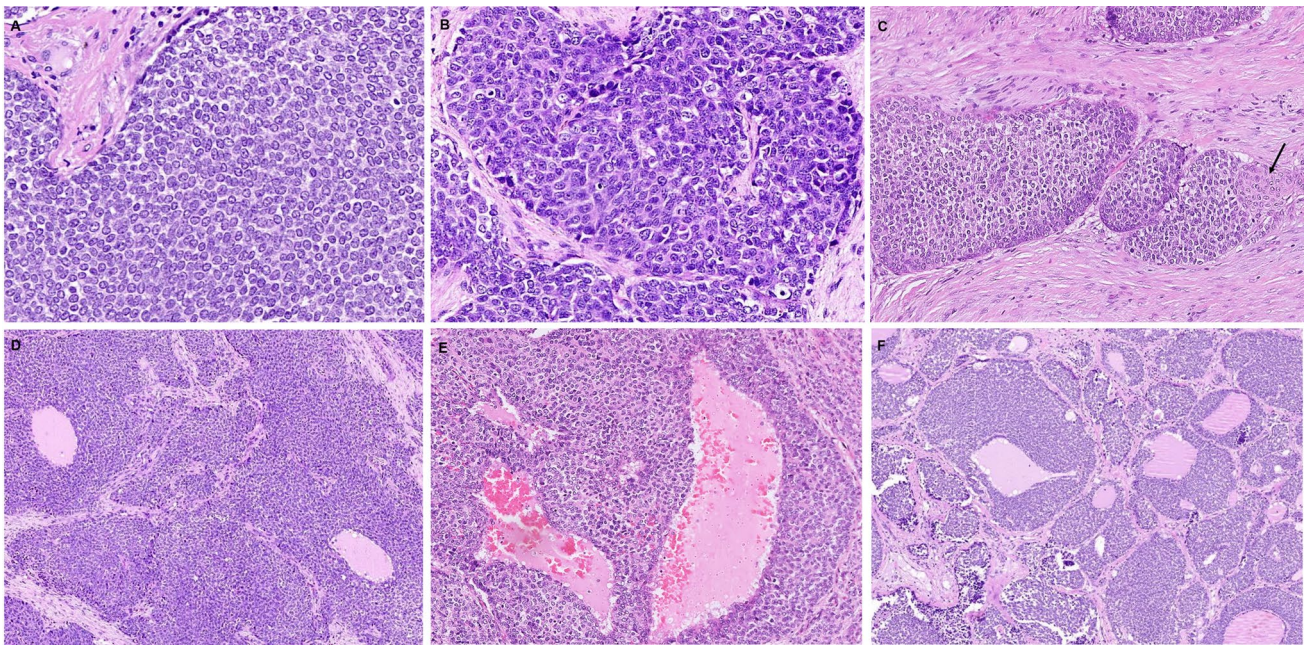


**Fig. 2** ALES tumor cells were monomorphic with predominant round cell (**A**) or basaloid morphology (**B**). Peripheral palisading was conspicuous in some tumor islands; the *arrow* highlights abrupt squamous differentiation (**C**). Follicle-like spaces filled with pale eosinophilic fluid were identified within the tumor nests and sheets in the nasal (**D**) and the parotid (**E**) tumors. Solid nests of tumor cells were admixed with follicles displaying variably thick collars of neoplastic cells replacing normal thyroid follicular cells in a clinging pattern while retaining luminal (colloid) secretions (**F**)

cellular fibrotic, or loose edematous, or partially myxoid. Mitotic activity and small foci of necrosis were frequent. The overlying mucosa was ulcerated by the tumor in 1 case. No intramucosal pagetoid spread was identified in any case. The underlying bone and cartilage involvement was present in 3 cases. Nodal metastasis was not observed.

Table 3 and Fig. 4 highlight the IHC characteristics of ALES cases. Briefly, the tumors exhibited a consistent

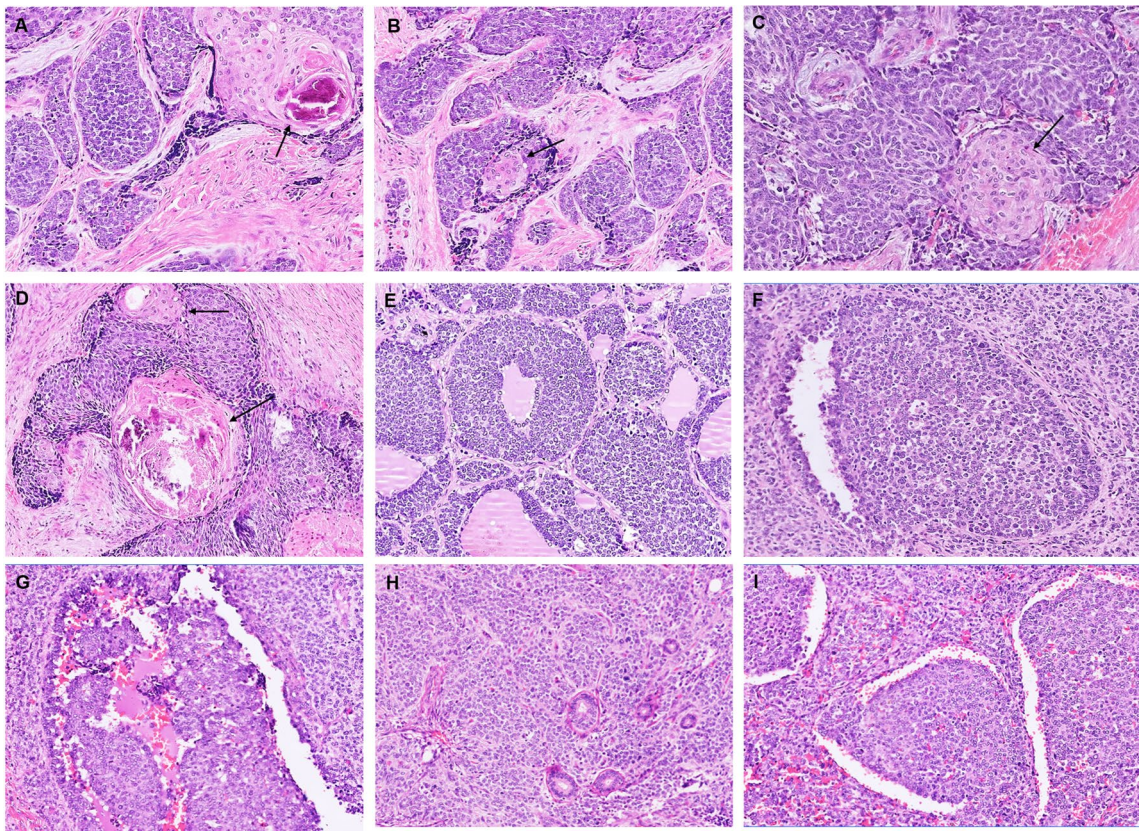


**Fig. 3** Squamous nests, eddies as well as larger keratinized squamous pearls were identified centered abruptly within the monotonous round cells; black arrows highlight the squamous nests. Many of the keratinous pearls were calcified (**A**–**D**). Other features included colonization of thyroid follicles by tumor cells (**E**), pagetoid spread of tumor cells into the salivary ducts (**F**, **G**), entrapped ducts (**H**), and cracking artifacts separating large tumor nests (**I**)

profile of diffuse cytokeratin, CD99 (membranous), p40/p63, NKX2.2, FLI-1, and focal synaptophysin positivity. Other markers, performed by the reporting pathologist to exclude a variety of differential diagnoses, including chromogranin, SMARCB1, p16, NUT, LCA, desmin, S100, PAX8, TTF1, WT1, BCOR, calretinin, and calcitonin were negative. Ki-67 ranged from 12–35%. All tumors were positive for *EWSR1* rearrangements on FISH (Fig. 4E, F).

## Adjuvant Treatment and Follow Up

Radiotherapy was administered to 4 patients (three adjuvant; one palliative). All patients received chemotherapy [EFT 2001 protocol; VAC/IE (vincristine + doxorubicin + cyclophosphamide and ifosfamide + etoposide) however one patient was lost to follow-up mid-treatment and did not return (case 3). The median follow-up was 26 months (range, 2–39 months; mean, 24.6 months). The response to therapy varied among the five patients who underwent treatment. One patient (case 2) remained disease-free after treatment at 26 months, while another (case 1) developed metastasis after a 36-month disease-free interval. The tumor showed excellent response to chemotherapy in case 6, however, the patient developed progressive disease after 24 months. Two patients developed local recurrences: one patient (case 4) abandoned treatment midway and returned with local recurrence, while the other (case 5) experienced an early recurrence. The time-to-recurrence was 10 and 6 months, respectively. Distant metastases were identified in three patients; the sites of metastasis included brain (in case 1), lung, and skeletal (in case 4), and pancreatic and skeletal (in case 6); the time-to-metastasis (measured from the end of curative treatment to the documentation of metastasis) was 25 months, 6 months, and 0 months, respectively. At the last follow-up visit, two patients were alive with no evidence of disease, three patients were alive with disease, while treatment was ongoing in one patient.

## Discussion

ALES is a rare variant of ES that is characterized by *EWSR1::FLI1* gene fusions and complex epithelial differentiation; the latter is defined by diffuse and intense

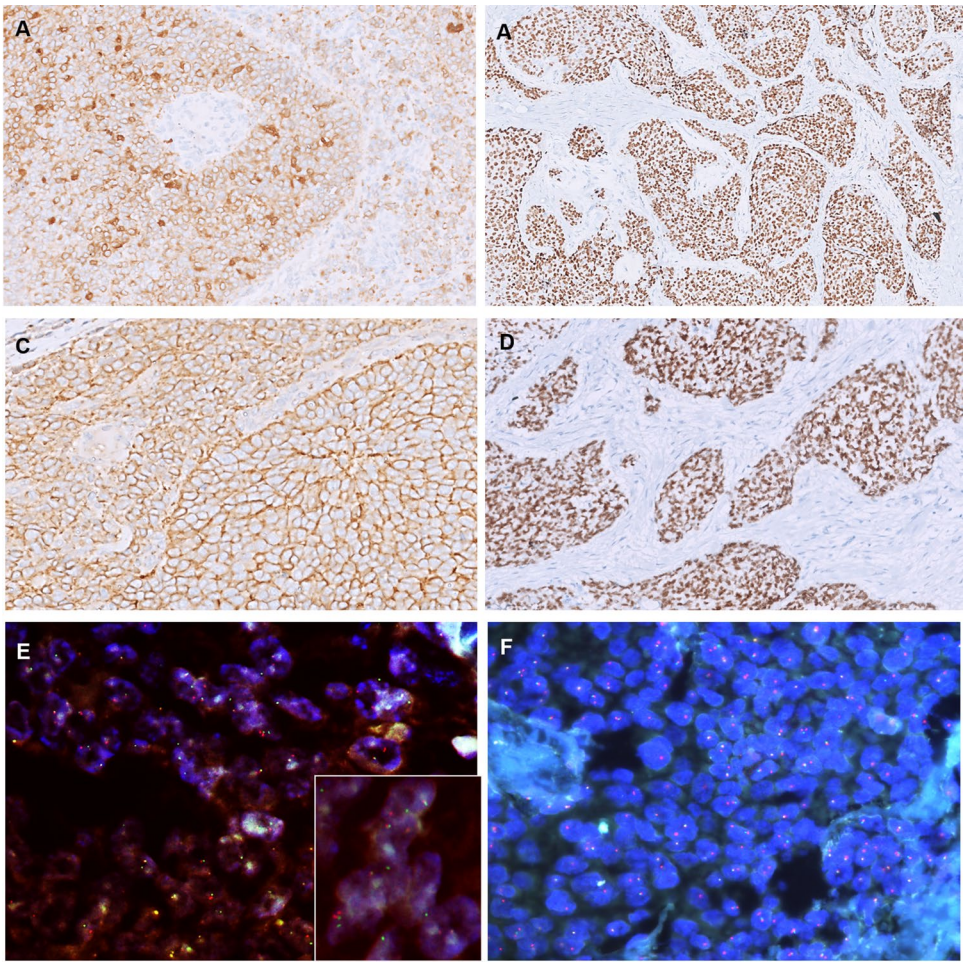


**Fig. 4** Immunohistochemistry of ALES. The tumor cells were strongly and diffusely positive for AE1/AE3 (**A**), p40 (**B**), CD99 (**C**), and NKX2.2 (**D**). Fluorescent in situ hybridization revealed *EWSR1* rearrangement (red-green 'spilt' signals in the inset, **E** E–F; DAPI × 1000)

immunoreactivity with multiple (high and low molecular weight) cytokeratins and both IHC and ultrastructural evidence of complex desmosomes and tonofilaments [2, 16]. Although ALES exhibits a proclivity to head and neck among other sites, accounting for about 74% of the cases, it is still a rare diagnosis with only 28 cases reported to date [3, 9, 14, 15, 18], summarized in Table 4. The sites previously reported include the major salivary glands (n = 12) [7–9], thyroid (n = 8) [4, 10–15], sinonasal tract (n = 4) [4–6], neck soft tissues (n = 3) [16–18], and orbit (n = 1) [4]. The previously reported cases include one case of head and neck ALES from our institute as a part of 34 cases of Ewing sarcoma with epithelial differentiation; the tumor arose in the neck soft tissues [18]. In the present study, we contribute seven additional cases of molecularly confirmed head and neck ALES (4 in sinonasal, 2 in parotid, and 1 in thyroid) and expand on the existing information on this rare malignancy.

While the age spectrum of ALES is wide (range 7–77 years), most (> 80%) patients are younger than 50 years of age (mean, 36.7 years; median, 36 years) [3–18]. Patients in our cohort were comparatively young, with an average age of 25.2 years (all were < 50 years of age). Site-wise age variations have been noted. The average age of salivary ALES patients has been observed to be greater than for non-salivary sites (49.3 years versus 25.8 years, respectively) [3–18]. Such site-specific age differences were, however, not appreciated in our small series. A minor male preponderance has been previously recorded (M: F, 1.2) [3–18], similar to our findings. Symptoms may be non-specific; most patients present with an enlarging mass, with or without pain, while sinonasal tumors mostly cause obstruction, pain, and/ or epistaxis. Rare instances of cervical sympathetic chain involvement leading to Horner syndrome and vocal cord palsy have been reported [16]. Exceptionally, metastatic disease may be the first presenting site. One of our patients presented with recurrent abdominal pain and was diagnosed as a solid pseudopapillary tumor in a pancreatic biopsy elsewhere. However, complete workup revealed a large primary in the maxilla and multiple skeletal and pancreatic metastases.

ALES may present with a variable tumor size that ranges from 2.2–7.9 cm [3, 4, 7, 9]. Macroscopic appearance usually reveals a grey-white tumor with a firm, lobulated

**Table 3** Ancillary testing in Adamantinoma-like Ewing Sarcoma cases (n = 7)

| Antibody | Case 1 | Case 2 | Case 3 | Case 4 | Case 5 | Case 5 | Case 6 | Case 7 |
|---|---|---|---|---|---|---|---|---|
| AE1/AE3 | + | + | + | + | + | + | + | + |
| EMA | ND | + | ND | ND | ND | ND | + | ND |
| p40 | + | + | + | + | + | + | + | + |
| CD99 (mic2) membranous | + | + | + | + | + | + | + | + |
| NKX2.2 | + | + | + | + | + | + | + | + |
| Fli1 | + | + | ND | + weak | ND | ND | + weak | + |
| Desmin | - | - | - | - | - | - | - | - |
| WT1 | ND | ND | ND | - | - | ND | - | - |
| Synaptophysin | + | + focal | - | - | + | - | + focal | + weak |
| Chromogranin | - | - | - | - | - | - | - | - |
| NUT | - | - | - | - | - | - | - | - |
| BCOR | - | ND | ND | ND | ND | ND | ND | - |
| TTF1 | - | ND | ND | ND | ND | ND | ND | ND |
| PAX8 | - | ND | ND | ND | ND | ND | ND | ND |
| Calcitonin | - | ND | ND | ND | ND | ND | ND | ND |
| Beta-catenin | ND | - | - | ND | ND | - | - | - |
| p16 diffuse (> 70%) | - | - | - | - | - | - | - | - |
| S100/ SOX10 | - | - | - | - | - | - | - | - |
| SMARCB1 | ND | ND | - | - | - | - | - | - |
| Ki67 labeling index | 12% | 28% | 30% | 35% | 15% | 30% | 25% | 18% |
| *EWSR1* break-apart FISH* | + | + | + | + | + | + | + | + |

*f* focal positivity (< 50% immunoreactivity), *ND* not done, *FISH* fluorescent in situ hybridization

*Ewing sarcoma break point region 1(EWSR1) (22q12.1)

cut surface and variable necrosis, calcification, and cystic change [3]. While most tumors may be organ confined, their borders tend to be infiltrative [3]. Histologic features of ALES are quite distinctive albeit encompassing a wide morphologic spectrum. Similar to ES, ALES is characterized by a monotonous population of round cells and CD99 (mic2) and NKX2.2 positivity. However, unlike typical ES, a nested growth pattern, peripheral palisading, and a complex epithelial differentiation (evinced by low- and high-molecular-weight cytokeratins, and p40/p63 immunoreactivity, with or without overt squamous differentiation, or keratin pearls) bestow ALES a deceptive resemblance to carcinomas [3, 4, 7]. These hybrid pathologic features of ES and carcinoma make ALES a distinctive and treacherous entity at the same time. Akin to most translocation-associated tumors, the neoplastic cells are characteristically monotonous and possess isomorphic nuclei, inconspicuous nucleoli, and scanty pale to basophilic, or clear cytoplasm [4, 7, 16]. Pseudo-rosettes are identified in more than half the cases, although their presence is usually focal [3, 4]. Tumors show brisk mitoses while necrosis is variable, ranging from sparse to extensive and geographic [16].

One of the distinctive features of diagnostic importance, identified in about a third of ALES cases [4–7, 9, 16, 17] is the presence of overt squamous differentiation. The latter may be present as rare isolated keratinized cells, or as variable-sized squamous nests, eddies, and sometimes as keratin pearls. Irrespective of their frequency, these squamous foci are conspicuous for their abrupt apposition to the monotonous round cells [4, 5, 7]. This appears to be least frequent at major salivary locations as about two-thirds of ALES cases with squamous differentiation have been reported at non-salivary sites [7]. Of our two cases with morphologic evidence of squamous differentiation, one was in the nasal cavity and the other in the parotid. Mixed architectural patterns comprising nests, lobules, trabeculae, and sheets are usually present with the nested pattern, even if focal, being consistent [4, 7]. Typically, these nests are separated by fibrous stroma which is mostly hyalinized and rarely may display a microcystic myxoid appearance [4]. Further, a subset of cases may display a hyaline basement membrane-like material which can erroneously sway the diagnosis towards a salivary gland tumor [4, 7]. Myxoid stroma or basement membrane-like material was not identified in any of our cases. Uncommonly, stromal osteo-fibrous dysplasia-like metaplasia [6], chondroid metaplasia [9], pseudoglandular pattern [17], vague streaming pattern [4], and a biphasic pattern with a spindle component have been described [17].

Another intriguing feature described by many authors is the peculiar colonization pattern of spread in ALES, documented in approximately 25% of cases [4, 6, 9, 13]. Rather

**Table 4** Site-wise literature on Adamantinoma-like Ewing Sarcoma

| Site | Author, year | Age/Sex | Initial diagnosis | Treatment S + XRT + CT | Locoregional Recurrence | Metastasis | Outcome | Follow up (months) |
|---|---|---|---|---|---|---|---|---|
| *Sinonasal region* | | | | | | | | |
| Nasal/ethmoid | Bishop et al. 2015 [4] | 37/F | PD SCC | Initially S; Recurrences: S + XRT + CT (docetaxel, carboplatin, capecitabine, methotrexate) | Yes; 24 months | Yes; Dural, 46 months | DWD | 52 |
| Ethmoid sinus, orbit, brain | Bishop 2015 [4] | 21/M | ALES | XRT + CT (VDC/IE) | Stable local disease | No | AWD | 12 |
| Nasal | Mahadevan 2019 [5] | 18/M | Basaloid SCa | NA | NA | NA | NA | NA |
| Nasal, maxilla, orbit | Alexiev 2017 [6] | 41/M | NUT Ca | S + CT (VDC/IE); RT pending | NA | NA | NA | 2 |
| Nasal | Bal 2021 [Present series] | 30/M | Basaloid SCC | S + XRT; CT at recurrence | Yes | Yes | AWD | 39 |
| Maxilla | Bal 2021 [Present series] | 27/M | Basaloid SCC | S + XRT + CT | Yes | No | AWD | 13 |
| Maxilla | Bal 2021 [Present series] | 25/F | Round cell tumor/solid pseudopapillary tumor | CT; Palliative RT | No | Pancreatic and skeletal metastasis (0 months) | AWD | 24 |
| Ethmoid/maxilla | Bal 2021 [Present series] | 34/F | SNEC | S; Additional therapy pending | NA | NA | NA | 0 |
| *Salivary* | | | | | | | | |
| Parotid | Lecanzo [8], Bishop 2015 [4] Rooper 2020 [7] | 56/F | Basal cell adenoca | S + XRT + CT (VDC/IE) | No | No | ANED | 1 |
| Parotid | Bishop 2015 [4]; Rooper 2020 [7] | 40/F | Basal cell adenoma | S; Additional therapy pending | NA | NA | NA | 0 |
| Parotid | Rooper 2020 [7] | 63/F | PD CA with basaloid features | S + CT (VDC/IE) | No residual | No | DWD | 3 |
| Parotid | Rooper 2020 [7] | 32/F | High grade neuroendocrine CA | S + XRT + CT (carboplatin/etoposide) | Persistent disease following initial therapy | No | AWD | 8 |
| Parotid | Rooper 2020 [7] | 32/M | PD CA with basaloid features | S + XRT + CT (VDC/IE) | No residual | No | ANED | 19 |
| Parotid | Rooper 2020 [7] | 41/M | PD CA with basaloid features | S + XRT + CT (initially carboplatin/paclitaxel then VDC/IE) | No residual | No | ANED | 24 |
| Parotid | Rooper 2020 [7] | 46/M | Merkel Cell Ca | S; additional treatment pending | No residual | No | NA | 0 |
| Parotid | Rooper 2020 [7] | 72/M | ALES | S; additional treatment pending | No residual | No | ANED | 1 |
| Parotid | Alnuaim 2020 [9] | 29/M | - | S + XRT + CT | Yes; 22 months | Pancreatic and skeletal metastasis (22 months) | AWD | 22 |

**Table 4** (continued)

| Site | Author, year | Age/Sex | Initial diagnosis | Treatment S + XRT + CT | Locoregional Recurrence | Metastasis | Outcome | Follow up (months) |
|---|---|---|---|---|---|---|---|---|
| Parotid | Alnuaim 2020 [9] | 46/F | PD NEC | S; additional therapy pending | NA | NA | NA | 3 |
| Submandibular | Rooper 2020 [7] | 77/M | PD CA with basaloid features | S + XRT + CT (doxorubicin) | No residual | No | ANED | 13 |
| Submandibular | Rooper 2020 [7] | 58/M | PD Ca | S; additional treatment pending | No residual | No | NA | 0 |
| Parotid | Bal 2021 [Present series] | 42/M | Basal cell adenoca | S | NA | NA | NA | 0 |
| Parotid | Bal 2021 [Present series] | 12/F | Sialoblastoma/ES | S + CT | NA | NA | ANED | 26 |
| *Thyroid* | | | | | | | | |
| Thyroid | Cruz [10]; Eloy [11] | 42/F | Small cell Ca | TT | NO | No | ANED | 38 |
| Thyroid | Eloy [11] | 24/M | PDTC | TT + XRT + CT | No | No | ANED | 156 |
| Thyroid | Bishop 2015 [4] | 19/M | ALES | S; additional therapy pending | NA | NA | NA | NA |
| Thyroid | Bishop 2015 [4] | 36/F | ALES | S; additional therapy pending | NA | NA | NA | NA |
| Thyroid | Ongkeko et al. [12] | 36/F | PDTC | S + XRT; CT at metastasis | No | Pancreatic 2 months | ANED | 24 |
| Thyroid | Morlete [13] | 20/F | ALES | TT + XRT + VDC | No | No | ANED | 7 |
| Thyroid | Jones 2020 [14] | 21/M | ALES | NA | NA | Multiple lytic bone lesions (? skeletal metastases) | NA | 0 |
| Thyroid | Taccogna 2021 [15] | 40/M | Undifferentiated thyroid carcinoma | TT | No | No | ANED | 9 |
| Thyroid | Bal 2021 [Present series] | 7/F | ES | HT + CT + RT | No | Brain, at 25 months | AWD | 32 |
| *Orbit* | | | | | | | | |
| Orbit | Bishop 2015 [4] | 7/F | Myoepithelial Ca | S + XRT + CT (ifosfamide + cyclophosphamide + etoposide, then ifosfamide + vincristine + etoposide) | No | No | ANED | 61 |
| *Neck soft tissues* | | | | | | | | |
| Neck ST and vagus | Weinreb [16] | 29/M | PDSCC | 66 Gy RT + 3# cisplatin. Later switched to VAC/IE | No | No | ANED | - |
| Vagus | Kikutchi [17] | 11/F | Malignant tumor | S + CT; S + RT (at recurrence) | Y | No | AWD | 36 |

**Table 4** (continued)

| Site | Author, year | Age/Sex | Initial diagnosis | Treatment S + XRT + CT | Locoregional Recurrence | Metastasis | Outcome | Follow up (months) |
|---|---|---|---|---|---|---|---|---|
| Neck soft tissues | Bharat Rekhi [18] | 36/M | - | S + XRT + CT | No | No | AWD | 17 |

*M* male, *F* female, *PDSCC* poorly differentiated squamous cell carcinoma, *S* surgery, *XRT* external beam radiotherapy, *Rt* radiotherapy, *CT* chemotherapy, *ALES* Adamantinoma-like Ewing Sarcoma, *Ca* carcinoma, *BSCC* basaloid squamous cell carcinoma, *SNEC* sinonasal neuroendocrine carcinoma, *ES* Ewing sarcoma, *PD Ca* poorly differentiated carcinoma, *TT* total thyroidectomy, *HT* hemithyroidectomy, *VDC/IE* alternating vincristine/doxorubicin/cyclophosphamide and ifosfamide/etoposide, *NA* not available, *DWD* died with disease, *AWD* alive with disease, *ANED* alive with no evidence of disease, *ST* soft tissues;

than a destructive infiltration into adjoining tissues, tumor cells display a clinging/ pagetoid pattern of spread along the pre-existing structures such as adjacent thyroid follicles, salivary ducts, and acini. This pattern has been most consistently reported in the thyroid where it may serve as a strong diagnostic clue (Figs. 1D, 2F, 3E.) [4, 13]. Similarly, an intraepithelial and intraductal pagetoid pattern of tumor spread, analogous to carcinomas, has been reported in the sinonasal mucosa [4, 6] and salivary ducts [9]. Further, some authors have described a permeative tumor cell infiltration with entrapment of normal ducts and thyroid follicles [11, 12]. We identified a similar colonization pattern of spread in two of our cases (Fig. 3F–G). Interestingly, follicle-like spaces formed by small cysts lined by neoplastic cells and filled with pale eosinophilic fluid were seen punctuating solid sheets in two of our non-thyroidal cases (Fig. 2D, E). Also, in one tumor a peculiar clefting artifact was seen rimming the coalescent nodules (Fig. 3I). Follicle-like spaces and clefting artifacts have not been previously reported in the literature and their significance as a specific finding remains to be seen. Lymphovascular invasion (LVI) has been identified in a few cases (~ 12%) [9, 10, 12]. Also, nerve infiltration has been observed in about one-third of cases [3, 4, 16, 17]; there are reports of facial nerve involvement in a parotid tumor [9] and vagus nerve infiltration in the neck tumors [16, 17]. We did not encounter nerve involvement or LVI in our cases. Two of our cases had R1 (microscopic margin positivity) resections. The impact of margins in ALES has not been evaluated adequately, although a complete resection seems logical. Lymph node involvement is remarkably low with most instances being reported at recurrences [12, 17]. None of our cases had regional lymph nodal involvement at presentation.

Rarity of occurrence leading to a lack of familiarity, exacerbated by overlap with diverse, and more frequently occurring pathologic entities make ALES particularly susceptible to misdiagnosis in the head and neck. The initial diagnosis in 20 out of 26 cases (where information is available) reported in the literature and 6 cases in the present series were erroneous (Table 4). On one hand, squamous differentiation, keratin pearls, basaloid cells, and peripheral palisading, renders ALES remarkably similar to carcinomas, especially basaloid squamous carcinoma or a poorly differentiated squamous cell carcinoma (SCC). Conversely, small round cell morphology of ALES can bring a plethora of small round cell tumors into the list of differential diagnoses, such as Ewing sarcoma (including *CIC*-rearranged sarcomas, *BCOR*-sarcomas, and round cell sarcomas with *EWSR1*-non-*ETS* fusions), lymphoma/leukemia, alveolar rhabdomyosarcoma, synovial sarcoma (poorly differentiated), melanoma, Merkel cell carcinoma, neuroendocrine carcinomas (NEC), and desmoplastic small round cell tumor (DSRCT), etc. [3, 4]. Furthermore, the tumor location brings

additional site-specific differential diagnoses into consideration. In the salivary gland (due to basaloid cells, basement membrane-like material, and palisading), ALES may mimic primary salivary neoplasms such as basal cell adenocarcinomas/adenomas (BCAC/BCA), myoepithelial neoplasms, solid adenoid cystic carcinoma, sialoblastoma, SCC, and NEC [3, 4]. Similarly, sinonasal ALES may be mistaken for basaloid/ poorly differentiated SCC, and NUT carcinoma (due to abrupt squamous differentiation/ keratinization) sinonasal NEC, sinonasal undifferentiated carcinoma, olfactory neuroblastoma, SMARCB1/SMARCA4-deficient carcinoma, HPV-multiphenotypic sinonasal carcinoma, or rarely, teratocarcinosarcoma (due to neuroectodermal and squamous elements in a biopsy). In the thyroid, poorly differentiated thyroid carcinoma, medullary thyroid carcinoma, and carcinoma with thymus-like elements (CASTLE) are the differential diagnoses. Periorbital soft tissue ALES can be mistaken for a sebaceous carcinoma, basal cell carcinoma, or basosquamous carcinoma. Rarely, hybrid features of neuroectodermal/endocrine and epithelial differentiation may be misdiagnosed as mixed neuroendocrine non-neuroendocrine neoplasm (MiNEN). Using appropriate ancillary tests can help in distinguishing ALES from its morphologic mimics. Table 5 highlights the IHC profiles and clinically relevant molecular alterations of the diverse histologic mimics of ALES at various sites.

ALES exhibits a characteristic immunoprofile of strong/ diffuse, membranous CD99 (mic2) and nuclear NKX2.2 positivity combined with diffuse and strong cytokeratin (including high-molecular-weight), p40, and p63 positivity [2–4]. Fli-1 and synaptophysin positivity (usually focal) may be seen in up to half the cases; the latter has been observed more frequently in salivary ALES (observed in 81% cases) [7]. While classic ES may demonstrate cytokeratin (mostly low molecular-weight) positivity in up to 25–30% cases [19–21], diffuse p40, p63, and HMWCK reactivity are not seen. Interestingly, variable p16 positivity, including diffuse [9], has been reported in ALES, however when investigated, no association with HPV has been discovered [4, 11]. ALES is consistently negative for NUT, desmin, LCA, SOX10, Melan A, SMA, WT1, BCOR, beta-catenin (nuclear), TLE1, PAX8, and TTF1 [2–4]. Ki67 labeling index ranges from 12–35% [6, 9]. p53 expression is usually wild type [16].

ALES share their molecular profile with classic ES that is defined by *FET::ETS* gene rearrangements [2]; the *FET* family of transcription factors include *EWSR1* or *FUS* and *TAF 15* while the *ETS* family comprises *FLI1, ERG, ETV1, E1A-F,* and *FEV* [2]. All cases of ALES have been reported to harbor the t(11;22) translocation with *EWSR1::FLI1* fusion by either FISH, reverse transcriptase-polymerase chain reaction (RT PCR), or next-generation sequencing [2, 3]. While this translocation or *EWSR1* rearrangement on break-apart FISH is diagnostic, it is noteworthy that many other distinct tumor entities, such as, myoepithelial carcinomas, hyalinizing clear cell carcinomas, *EWSR1*-non-*ETS* sarcomas, and DSRCT may also harbor *EWSR1* rearrangement [3]. Conversely, it is plausible that genes other than *EWSR1*, such as *FUS*, or *TAF-15* belonging to the *FET* family may be involved, although this has not been reported so far for ALES. Two of our cases (not included in the present study) with classical histopathologic and IHC features of ALES were negative for *EWSR1* break-apart FISH. However, a lack of further investigation precluded the determination of the underlying genetic alteration.

Knowledge of the clinical course of ALES and the optimal treatment is limited as few studies are available with long-term follow-up. Most patients of ALES have received multi-modality treatment comprising surgery, RT, and CT; latter usually on the lines of ES treatment using VAC or VDC alternating with IE [3]. Out of 26 previously published cases, treatment and outcome information is available in only 18 patients with a median follow-up duration of 13 months (mean 26.7 months; range 7–156 months) [3–18]. Of these 18 patients, local recurrences/persistent disease was noted in 27.8% of patients while 17% of patients developed distant metastasis [3–18]. The sites of metastasis reported were dura [4], pancreas, and skeletal [9, 12]. Two-thirds were alive with no evidence of disease, 22.2% were alive with the disease while 11.1% had died of the disease [3–18]. Among our patients, the recurrence rate was 33.3% while three (50%) of our patients developed disseminated disease with sites of metastases being brain, pancreas, skeleton, and lung. In our study with a median follow-up of 26 months, 40% of patients were alive with no evidence of disease while 60% were alive with the disease. In our small cohort of patients treated with multimodality treatment, the high rate of disease relapse suggests aggressive biology. Studies on larger patient cohorts are warranted to decipher the long-term outcomes of this rare malignancy.

Our study had limitations of a retrospective study, a small sample size, and inadequate follow-up. Nonetheless, the present study adds seven additional cases of a rare malignancy that further expands the knowledge of the morphologic and clinical spectrum of ALES while underscoring the need to avoid diagnostic errors. To the best of our knowledge, this is the largest study from the South-Asian region in the Indian population. We also report for the first time the presence of follicle-like spaces in these tumors that may serve as a useful diagnostic clue.

## Conclusion

ALES is a rare malignancy with distinctive pathologic features and a strong predilection for the head and neck region. Nested architecture, cellular monotony, complex

**Table 5** Ancillary testing in differential diagnoses of Adamantinoma-like Ewing Sarcoma

| Tumor | Immunophenotype | Clinically relevant Molecular alterations | References |
|---|---|---|---|
| Adamantinoma-like Ewing Sarcoma | CD99, NKX2.2, AE1/AE3, p40, p63, HMWCK, Fli1 (v), Synaptophysin (v), Chromogranin (v), p16 (v) | *EWSR1::FLI1* | [2–18, 22] |
| Predominantly round cell morphology [2, 19–30] | | | |
| Classic Ewing sarcoma | CD99 (membranous), NKX2.2, Fli1 (fusion pos), ERG (fusion pos), AE1/AE3 (25%), S100 (-/+) | *EWSR1::FLI1* ((about 85%), *EWSR1::ERG* (about 10%), others members of *FET* (*TAF15, FUS, EWSR1*) and *ETS* family | [2, 19–22] |
| Sarcoma with BCOR | BCOR, SATB2, TLE1, cyclin D1, CD99 (50%) | *BCOR* rearrangements (mostly, *BCOR::CCNB3*); *BECOR*-ITD | [22, 23] |
| CIC-related sarcoma | WT1, CD99 (focal; 20% diffuse), ETV-4, calretinin (v), ERG (v)<br>Occ pos-Keratins, S100, desmin;<br>CIC-NUTM1 express NUT<br>NKX2.2 is negative | *CIC::DUX4* (95%); *CIC::NUTM1* | [22, 24, 25] |
| Round cell sarcoma with EWSR1-non-ETS | Variable co-expression of myogenic markers (desmin, myogenin, MYOD1) and neurogenic markers (S100P, SOX10, MITF, GFAP)<br>CD34 can be positive<br>CD99 is not consistently expressed | *EWSR1::NFATC2, FUS::NFATC2, and EWSR1::PATZ1* | [22, 26, 27] |
| Alveolar Rhabdomyosarcoma | Desmin, Myogenin, MyoD1, CD99 (cytoplasmic ±),<br>Occ pos- AE1/AE3, synaptophysin, chromogranin, CD56 (pitfall) | 85% fusion; *PAX3::FOXO1* (70–90%); *PAX7::FOXO1* (10–30%) | [22, 28] |
| Desmoplastic small round cell tumor | AE1/AE3, desmin, WT1 (C-terminus antibody), NSE, CD56, CD99 (v)<br>Myogenin and MYOD1 are consistently negative | *EWSR1* gene rearrangement; *EWSR1::WT1* fusion | [22, 29] |
| Non-Hodgkin Lymphoma/ Leukemia | LCA, B cell or T cell lineage markers, Tdt (leukemic blasts) | Lymphoma specific gene fusions | [22] |
| Poorly differentiated Synovial sarcoma | EMA, keratins, SS18-SSX fusion specific antibody, TLE1, bcl-2, CD99 (v), S100 (v, focal) | *SS18::SSX1/2/4* | [22, 30] |
| Predominantly neuroendocrine/ neuroectodermal | | | |
| Olfactory neuroblastoma | Synaptophysin, chromogranin, SSTR2, calretinin, AE1/AE3 (-/+, 1/3rd focal), S100 positive rim<br>Negative- CD99 | – | [31] |
| Sinonasal neuroendocrine carcinoma | AE1/AE3, Synaptophysin, chromogranin | | [3, 4] |
| Teratocarcinosarcoma (in a biopsy; sampling of the neuroectodermal components) | Neuroectodermal component-CD99 (cytoplasmic), synaptophysin, INSM1, Chromogranin (v), GFAP (v)<br>Squamous- p40/p63 +<br>Epithelial- AE1/AE3, Ck7 (v)<br>Mesenchymal- Vimentin, desmin (v), MyoD1 (v) | *SMARCA4* deletions (subset) | [32] |
| Melanoma | HMB45, S100, SOX10, Melan A, TIFF | *KIT, RAS, BRAF* mutations | [33] |
| Merkel cell carcinoma | Cytokeratins, synaptophysin, chromogranin, NSE, INSM1, CD56, NFP, CK20 (perinuclear dot), CM2B4 (anti-MCPyV) | MCPyV DNA | [3, 4, 34] |
| Predominantly carcinoma morphology | | | |
| Basaloid squamous carcinoma | Cytokeratins, p40, p63, HMWCK | – | [3, 4] |
| NUT carcinoma | NUT, AE1/AE3, p63 > p40, HMWCK, synaptophysin and, chromogranin (occasional), CD34 (v) | *NUT::BRD4; NUT::BRD3; NUT::NSD3;* | [35] |

**Table 5** (continued)

| Tumor | Immunophenotype | Clinically relevant Molecular alterations | References |
|---|---|---|---|
| SMARCB1-deficient carcinoma | SMARCB1 loss, AE1/AE3, p40, p63, HMWCK, CK7 (v)<br>Synaptophysin and chromogranin (v, 8–18%) | Biallelic *SMARCB1* deletions (2/3rds) | [4, 36] |
| SMARCA4-deficient carcinoma | SMARCA4 loss, AE1/AE3, CK7 (rare), synaptophysin (90%), chromogranin (40%), CD56 (60%) | Biallelic *SMARCA4* inactivation | [4, 36] |
| Sinonasal undifferentiated carcinoma | AE1/AE3, CK7, p63 (v), p16 (v), IDH1/2 mutant specific (subset) | *IDH2*-mutations (33–85%) | [3, 4, 37] |
| Basal cell adenocarcinoma | Cytokeratins, p40, p63, S100, SOX10, beta-catenin | *CYLD* or *CTNNB1* alterations (subset) | [7, 38] |
| Myoepithelial carcinoma | Cytokeratins, p40, p63, S100, SOX10, SMA, calponin | *EWSR1::POU5F1, PBX1, PBX3 or ZNF444*<br>*Clear cell MECA- EWSR1 rearrangements* | [7, 39] |
| Sialoblastoma | Cytokeratins (v), SOX10, p63, beta-catenin, S100 (v), SMA (v), CD117 (v), and calponin (v) | – | [40] |
| Solid Adenoid cystic carcinoma | Cytokeratins, CK7, SOX10, S100, SMA, p40, p63, Calponin | *MYB/MYBL1* gene rearrangements or fusions | [4, 7, 41] |
| Ameloblastic Carcinoma | Cytokeratins, p40, p63, CK19, calretinin, SOX2 (v), SMA (v), abnormal p53 | *BRAF V600E; TP53* | [42] |
| Sebaceous carcinoma | EMA, p40, p63, p16, AR, adipophylin, p53, perilipin | *TP53/RB1* mutations; *HER2* amplification (75%) | [43, 44] |
| Basal cell carcinoma/basosquamous carcinoma | BerEP4, p40, p63, bcl-2, synaptophysin (v), chromogranin (v) | – | [45] |
| Mixed neuroendocrine non-neuroendocrine neoplasm (MiNEN) | Synaptophysin, chromogranin, INSM1 in the NE component;<br>Cytokeratins in non-NE, p40 if squamous component | – | [46] |
| Medullary thyroid Carcinoma | Calcitonin, INSM1, Synaptophysin, Chromogranin, CEA, TTF1 (v) | *RET* gene rearrangements | [47] |
| Poorly differentiated thyroid carcinoma | AE1/AE3, TTF1, PAX8, Thyroglobulin positive | – | [3, 4] |
| CASTLE | CD5, p63, CD117, synaptophysin (v), chromogranin (v) | – | [3, 48] |

*v* variable positivity, *pos* positive, *ITD* Internal tandem duplication, *occ* occasional, *NE* neuroendocrine, *CASTLE* Carcinoma with thymus-like elements;

epithelial differentiation, and *EWSR1::FLI1* translocation are the pathologic hallmarks of ALES. The peculiar tendency towards the colonization of native structures and the presence of follicle-like spaces may serve as useful diagnostic clues. Further, the awareness that abrupt squamous differentiation with keratinization is a feature seen in a subset of ALES may avert diagnostic pitfalls when interpreting head and neck tumor biopsies. Whether ALES belongs with ES or is an independent entity sharing the same translocation is debatable. Nonetheless, ALES displays a unique set of pathologic features that make it a distinctive clinicopathologic entity. Its biology and optimal treatment protocols need to be defined and warrant larger prospective multicentric studies.

**Supplementary Information** The online version contains supplementary material available at https://doi.org/10.1007/s12105-022-01412-1.

**Author Contributions** The study conception and design were by Munita Bal. Provision of study materials or patients: Munita Bal, Aekta Shah, Neha Mittal, Katha Rabade, Swapnil Rane, Gauri Pantavaidya, Deepa Nair, Sarbani Ghosh Laskar, Siddharth Laskar, Aishwarya Malla, Krishna Kumar, Prabhash Kumar. Collection and assembly of data: Munita Bal, Aekta Shah. Data analysis and interpretation: Munita Bal, Asawari Patil, Aekta Shah, Bharat Rekhi, Omshree Shetty. The first draft of the manuscript was written by Munita Bal and all authors commented on previous versions of the manuscript. All authors read and approved the final manuscript.

**Funding** No funding obtained.

## Declarations

**Conflict of interest** No conflict of interest to disclose.

**Ethical Approval** All procedures performed in the study were in accordance with the ethical standards of the Institutional Ethics Committee (IEC). A waiver of review was granted by the IEC after due examination.

**Informed Consent** Not required as per institutional ethics committee's policy for retrospective case series. The authors declare that all information is anonymized and the submission does not include images that may identify any patient.

## References


1. Bridge JA, Fidler ME, Neff JR, Degenhardt J, Wang M, Walker C, et al. Adamantinoma-like Ewing's sarcoma: genomic confirmation, phenotypic drift. Am J Surg Pathol. 1999;23:159–65.
2. de Alava E, Lessnick SL, Stamenkovic I. Tumors of uncertain differentiation/Ewing sarcoma. In: World Health Organization (WHO) classification of tumours editorial board, eds. World Health Organization classification of tumours. 5th edition. Soft tissue and bone tumours. Lyon, France: IARC Press; 2020: 323–5.
3. Rooper LM, Bishop JA. Soft Tissue Special Issue: Adamantinoma-Like Ewing Sarcoma of the Head and Neck: A Practical Review of a Challenging Emerging Entity. Head Neck Pathol. 2020;14:59–69.
4. Bishop JA, Alaggio R, Zhang L, Seethala RR, Antonescu CR. Adamantinoma-like Ewing family tumors of the head and neck: a pitfall in the differential diagnosis of basaloid and myoepithelial carcinomas. Am J Surg Pathol. 2015;39:1267–74.
5. Mahadevan P, Ramkumar S, Gangadharan VP. Adamantinoma-Like Ewing's family tumor of the sino nasal region: a case report and a brief review of literature. Case Rep Pathol. 2019;2019:6.
6. Alexiev BA, Tumer Y, Bishop JA. Sinonasal adamantinoma-like Ewing sarcoma: a case report. Pathol Res Pract. 2017;213:422–6.
7. Rooper LM, Jo VY, Antonescu CR, Nose V, Westra WH, Seethala RR, Bishop JA. Adamantinoma-like Ewing sarcoma of the salivary glands: a newly recognized mimicker of basaloid salivary carcinomas. Am J Surg Pathol. 2019;43:187–94.
8. Lezcano C, Clarke MR, Zhang L, Antonescu CR, Seethala RR. Adamantinoma-like Ewing sarcoma mimicking basal cell adenocarcinoma of the parotid gland: a case report and review of the literature. Head Neck Pathol. 2015;9:280–5.
9. Alnuaim H, Alzahrani M, Ghandurah S, Dababo M. Adamantinoma-like ewing sarcoma of the parotid gland: report of two cases and review of literature. Cureus. 2020;12:e11870.
10. Cruz J, Eloy C, Aragues JM, Vinagre J, Sobrinho-Simoes M. Small-cell (basaloid) thyroid carcinoma: a neoplasm with a solid cell nest histogenesis? Int J Surg Pathol. 2011;19:620–6.
11. Eloy C, Oliveira M, Vieira J, Teixeira MR, Cruz J, Sobrinho-Simoes M. Carcinoma of the thyroid with ewing family tumor elements and favorable prognosis: report of a second case. Int J Surg Pathol. 2014;22:260–5.
12. Ongkeko M, Zeck J, de Brito P. Molecular testing uncovers an Adamantinoma-like Ewing family of tumors in the thyroid: case report and review of literature. AJSP Rev Rep. 2018;23:8–12.
13. Morlote D, Harada S, Lindeman B, Stevens TM. Adamantinoma-like Ewing sarcoma of the thyroid: a case report and review of the literature. Head Neck Pathol. 2019;13:618–23.
14. Jones R, Maleki Z. Adamantinoma-like Ewing sarcoma of the thyroid. Diagn Cytopathol. 2020;48:E4–6.
15. Taccogna S, Guglielmi R, Persichetti A, et al. Carcinomas of the thyroid with Ewing family tumor elements (CEFTEs): a diagnostic challenge before surgery. Head Neck Pathol. 2021;15:254–61.
16. Weinreb I, Goldstein D, Perez-Ordoñez B. Primary extraskeletal Ewing family tumor with complex epithelial differentiation: a unique case arising in the lateral neck presenting with Horner syndrome. Am J Surg Pathol. 2008;32:1742–8.
17. Kikuchi Y, Kishimoto T, Ota S, Kambe M, Yonemori Y, Chazono H, Yamasaki K, Ochiai H, Hiroshima K, Tanaka M, Tanaka Y, Horie H, Nakatani Y. Adamantinoma-like Ewing family tumor of soft tissue associated with the vagus nerve: a case report and review of the literature. Am J Surg Pathol. 2013;37:772–9.
18. Rekhi B, Shetty O, Vora T, Gulia A, Bajpai J, Laskar S. Clinicopathologic, immunohistochemical, molecular cytogenetic profile with treatment and outcomes of 34 cases of Ewing sarcoma with epithelial differentiation, including 6 cases with "Adamantinoma-like" features, diagnosed at a single institution in India. Ann Diagn Pathol. 2020;49:151625.
19. Folpe AL, Goldblum JR, Rubin BP, Shehata BM, Liu W, Dei Tos AP, et al. Morphologic and immunophenotypic diversity in Ewing family tumors: a study of 66 genetically confirmed cases. Am J Surg Pathol. 2005;29:1025–33.
20. Collini P, Sampietro G, Bertulli R, Casali PG, Luksch R, Mezzelani A, et al. Cytokeratin immunoreactivity in 41 cases of ES/PNET confirmed by molecular diagnostic studies. Am J Surg Pathol. 2001;25:273–4.
21. Gu M, Antonescu CR, Guiter G, Huvos AG, Ladanyi M, Zakowski MF. Cytokeratin immunoreactivity in Ewing's sarcoma: prevalence in 50 cases confirmed by molecular diagnostic studies. Am J Surg Pathol. 2000;24:410–6.
22. WHO Classification of Tumours Editorial Board. Soft tissue and bone tumours. Lyon: International Agency for Research on Cancer; 2020.
23. Kao YC, Owosho AA, Sung YS, Zhang L, Fujisawa Y, Lee JC, Wexler L, Argani P, Swanson D, Dickson BC, Fletcher CDM, Antonescu CR. BCOR-CCNB3 fusion positive sarcomas: a clinicopathologic and molecular analysis of 36 cases with comparison to morphologic spectrum and clinical behavior of other round cell sarcomas. Am J Surg Pathol. 2018;42:604–15.
24. Yoshida A, Goto K, Kodaira M, Kobayashi E, Kawamoto H, Mori T, Yoshimoto S, Endo O, Kodama N, Kushima R, Hiraoka N, Motoi T, Kawai A. CIC-rearranged sarcomas: a study of 20 cases and comparisons with Ewing sarcomas. Am J Surg Pathol. 2016;40:313–23.
25. Kawamura-Saito M, Yamazaki Y, Kaneko K, Kawaguchi N, Kanda H, Mukai H, Gotoh T, Motoi T, Fukayama M, Aburatani H, Takizawa T, Nakamura T. Fusion between CIC and DUX4 up-regulates PEA3 family genes in Ewing-like sarcomas with t(4;19)(q35;q13) translocation. Hum Mol Genet. 2006;15:2125–37.
26. Wang GY, Thomas DG, Davis JL, Ng T, Patel RM, Harms PW, Betz BL, Schuetze SM, McHugh JB, Horvai AE, Cho SJ, Lucas DR. EWSR1-NFATC2 translocation-associated sarcoma clinicopathologic findings in a rare aggressive primary bone or soft tissue tumor. Am J Surg Pathol. 2019;43:1112–22.
27. Chougule A, Taylor MS, Nardi V, Chebib I, Cote GM, Choy E, Nielsen GP, Deshpande V. Spindle and round cell sarcoma with EWSR1-PATZ1 gene fusion: a sarcoma with polyphenotypic differentiation. Am J Surg Pathol. 2019;43:220–8.
28. Thompson LDR, Jo VY, Agaimy A, et al. Sinonasal tract alveolar rhabdomyosarcoma in adults: a clinicopathologic and immunophenotypic study of fifty-two cases with emphasis on epithelial immunoreactivity. Head Neck Pathol. 2018;12:181–92.
29. Barnoud R, Sabourin JC, Pasquier D, Ranchère D, Bailly C, Terrier-Lacombe MJ, Pasquier B. Immunohistochemical expression of WT1 by desmoplastic small round cell tumor: a comparative

study with other small round cell tumors. Am J Surg Pathol. 2000;24:830–6.
30. Baranov E, McBride MJ, Bellizzi AM, Ligon AH, Fletcher CDM, Kadoch C, Hornick JL. A novel SS18-SSX fusion-specific antibody for the diagnosis of synovial sarcoma. Am J Surg Pathol. 2020;44:922–33.
31. Cracolici V, Wang EW, Gardner PA, Snyderman C, Gargano SM, Chiosea S, Singhi AD, Seethala RR. SSTR2 expression in olfactory neuroblastoma: clinical and therapeutic implications. Head Neck Pathol. 2021;15:1185–91.
32. Rooper LM, Uddin N, Gagan J, Brosens LAA, Magliocca KR, Edgar MA, Thompson LDR, Agaimy A, Bishop JA. Recurrent loss of SMARCA4 in sinonasal teratocarcinosarcoma. Am J Surg Pathol. 2020;44:1331–9.
33. Nassar KW, Tan AC. The mutational landscape of mucosal melanoma. Semin Cancer Biol. 2020;61:139–48.
34. Busam KJ, Jungbluth AA, Rekthman N, et al. Merkel cell polyomavirus expression in merkel cell carcinomas and its absence in combined tumors and pulmonary neuroendocrine carcinomas. Am J Surg Pathol. 2009;33:1378–85.
35. Stevens TM, Morlote D, Xiu J, Swensen J, Brandwein-Weber M, Miettinen MM, Gatalica Z, Bridge JA. NUTM1-rearranged neoplasia: a multi-institution experience yields novel fusion partners and expands the histologic spectrum. Mod Pathol. 2019;32:764–73.
36. Agaimy A, Bishop JA. SWI/SNF-deficient head and neck neoplasms: an overview. Semin Diagn Pathol. 2021;38:175–82.
37. Dogan S, Chute DJ, Xu B, Ptashkin RN, Chandramohan R, Casanova-Murphy J, Nafa K, Bishop JA, Chiosea SI, Stelow EB, Ganly I, Pfister DG, Katabi N, Ghossein RA, Berger MF. Frequent IDH2 R172 mutations in undifferentiated and poorly-differentiated sinonasal carcinomas. J Pathol. 2017;242:400–8.
38. Jo VY, Sholl LM, Krane JF. Distinctive patterns of CTNNB1 (β-Catenin) alterations in salivary gland basal cell adenoma and basal cell adenocarcinoma. Am J Surg Pathol. 2016;40:1143–50.
39. Skálová A, Weinreb I, Hyrcza M, Simpson RH, Laco J, Agaimy A, Vazmitel M, Majewska H, Vanecek T, Talarčik P, Manajlovic S, Losito SN, Šteiner P, Klimkova A, Michal M. Clear cell myoepithelial carcinoma of salivary glands showing EWSR1 rearrangement: molecular analysis of 94 salivary gland carcinomas with prominent clear cell component. Am J Surg Pathol. 2015;39:338–48.
40. Li B, Jie W, He H. Myb immunohistochemical staining and fluorescence in situ hybridization in salivary rare basaloid lesions. Front Oncol. 2020;10:870.
41. Mitani Y, Liu B, Rao PH, Borra VJ, Zafereo M, Weber RS, Kies M, Lozano G, Futreal PA, Caulin C, El-Naggar AK. Novel MYBL1 gene rearrangements with recurrent MYBL1-NFIB fusions in salivary adenoid cystic carcinomas lacking t(6;9) translocations. Clin Cancer Res. 2016;22:725–33.
42. Niu Z, Li Y, Chen W, Zhao J, Zheng H, Deng Q, Zha Z, Zhu H, Sun Q, Su L. Study on clinical and biological characteristics of ameloblastic carcinoma. Orphanet J Rare Dis. 2020;15:316.
43. Muthusamy K, Halbert G, Roberts F. Immunohistochemical staining for adipophilin, perilipin and TIP47. J Clin Pathol. 2006;59:1166–70.
44. Kwon MJ, Shin HS, Nam ES, Cho SJ, Lee MJ, Lee S, Park HR. Comparison of HER2 gene amplification and KRAS alteration in eyelid sebaceous carcinomas with that in other eyelid tumors. Pathol Res Pract. 2015;211:349–55.
45. Houcine Y, Chelly I, Zehani A, Belhaj Kacem L, Azzouz H, Rekik W, Hend C, Haouet S, Kchir N. Neuroendocrine differentiation in basal cell carcinoma. J Immunoassay Immunochem. 2017;38:487–93.
46. Bal MM, Hubale B, Janu A, Patil A. Salivary duct carcinoma and small cell carcinoma ex-pleomorphic adenoma: a heretofore undescribed entity and the naming conundrum: MiNEN, combined, collision, or composite tumor? Oral Surg Oral Med Oral Pathol Oral Radiol. 2021;132:e92–6.
47. Hedayati M, Zarif Yeganeh M, Sheikholeslami S, Afsari F. Diversity of mutations in the RET proto-oncogene and its oncogenic mechanism in medullary thyroid cancer. Crit Rev Clin Lab Sci. 2016;53:217–27.
48. Kakudo K, Bai Y, Ozaki T, Homma K, Ito Y, Miyauchi A. Intrathyroid epithelial thymoma (ITET) and carcinoma showing thymus-like differentiation (CASTLE): CD5-positive neoplasms mimicking squamous cell carcinoma of the thyroid. Histol Histopathol. 2013;28:543–56.